Analysis of Beam-Beam Interactions with a Large Crossing Angle

Kohji Hirata*
Stanford Linear Accelerator Center, Stanford University, Stanford, California 94309
(Received 25 October 1993)

The beam-beam interaction for a flat beam with a large horizontal crossing angle is studied for the case in which the vertical betatron function at the interaction point is comparable to the bunch length. It is shown that crossing with a large angle has less serious detrimental effects than is usually believed. A large crossing angle might have several merits for future high-luminosity colliding rings.

PACS numbers: 41.85.–p, 29.27.Bd, 41.75.Ht

Nowadays, high-luminosity e^+e^- colliding rings are being considered seriously. Small bunch spacing is useful because collisions occur more frequently. This causes the problem of parasitic collisions: Bunches may interact with each other not only at the interaction point (IP) but also at points around the IP. These can be avoided by collision with a crossing angle. This, however, leads to another difficulty. The collision with a crossing angle causes an instability due to the synchrobetatron (SB) resonances which are known to have limited the performance of the DORIS collider [1]. It is widely believed that SB resonances become more serious for larger crossing angles [2].

The vertical betatron function at the IP (β_y^0) considered in recent designs is much smaller than traditional ones and is comparable to the bunch length σ_z. The analysis of the head-on collision for this case [3] has shown that the SB resonances are weakened by the bunch-length effect. This can easily be tested in simulation in which a bunch is split into several longitudinal slices. In this Letter, we study the bunch-length effects in the collision with a crossing angle [4]. We develop a new method of calculation. One ingredient is the mapping, called synchrobeam mapping (SBM), which is symplectic in a six-dimensional sense but is formulated only for the head-on collision [5]. The other is a Lorentz transformation that transforms the collision with an angle to a head-on collision [6] between bunches tilted horizontally (see Fig. 1). Thanks to the six-dimensional nature of the SBM, it is relatively easy.

Model.—We assume one IP in a ring located at $s = 0$, where s is the azimuthal coordinate. At the IP, coordinates of a particle are boosted so that the collision becomes head-on ($\mathcal{L}$). then the particle interacts with the other beam in this boosted frame in which the SBM is used. The particle is then transformed back to the original frame ($\mathcal{L}^{-1}$). It is transformed from IP to IP by betatron and synchrotron oscillations with radiation damping and excitation ($\mathcal{A}$). We denote the variables of each step as follows:

$$\mathbf{x}(0) \xrightarrow{\mathcal{L}} \mathbf{x}^*(0^*) \xrightarrow{\text{SBM}} \mathbf{x}^{*\prime}(0^*) \xrightarrow{\mathcal{L}^{-1}} \mathbf{x}'(0) \xrightarrow{\mathcal{A}} \mathbf{x}(0) \cdots .$$

We always transform quantities at $s = 0$ to those defined at $s = 0$.

We employ the coordinate system $\mathbf{x} = (x, p_x, y, p_y, z, p_z; h, s)$ called the accelerator coordinate. Here x and y are horizontal and vertical coordinates, respectively, and their conjugate momenta are defined as $(p_x, p_y) = m\gamma(dx/ds, dy/ds)/P_0$, where P_0 is the absolute value of the three-momentum $\mathbf{P}$ of the reference particle, m is the mass of the electron, and γ is the relativistic Lorentz factor. We use $z = s - ct(s)$, where c is the light velocity, t the arrival time at the position s, and $p_z = (|\mathbf{P}| - P_0)/P_0$. The h is the "Hamiltonian:" We use

$$h(p_x, p_y, p_z) = p_z + 1 - \sqrt{(p_z + 1)^2 - p_x^2 - p_y^2}. \quad (1)$$

This is the momentum along the reference trajectory, and s is the "time," which is the position in the ring. Here we take the ultrarelativistic limit.

Lorentz Boost $\mathcal{L}$.—We perform a Lorentz transformation for the Cartesian coordinate: $\mathbf{X} = (X, Y, Z, P_X, P_Y, P_Z; H, T)$, which is defined for the laboratory frame. Here H is the true Hamiltonian, which is the energy, and T is the time. The relations between the accelerator coordinates are

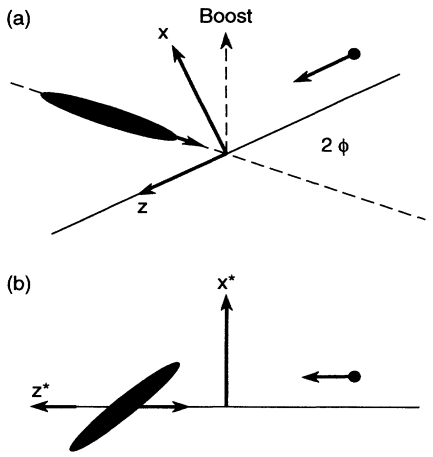

FIG. 1. Beams colliding at an angle in the original frame (a) and in the boosted frame (b). The coordinate frames are also shown. The direction of the Lorentz boost $\mathcal{L}$ is indicated by a dotted line.

 0031-9007/95/74(12)/2228(4)$06.00

$$\begin{pmatrix} cT \\ X \\ Z \\ Y \end{pmatrix} = \underbrace{\begin{pmatrix} -1 & 0 & 1 & 0 \\ 0 & 1 & 0 & 0 \\ 0 & 0 & 1 & 0 \\ 0 & 0 & 0 & 1 \end{pmatrix}}_{A} \begin{pmatrix} z(s) \\ x(s) \\ s \\ y(s) \end{pmatrix},$$

and

$$P_0 \begin{pmatrix} p_z \\ p_x \\ h \\ p_y \end{pmatrix} = \underbrace{\begin{pmatrix} 1 & 0 & 0 & 0 \\ 0 & 1 & 0 & 0 \\ 1 & 0 & -1 & 0 \\ 0 & 0 & 0 & 1 \end{pmatrix}}_{B} \begin{pmatrix} H/c - P_0 \\ P_X \\ P_Z - P_0 \\ P_Y \end{pmatrix}.$$

The Lorentz boost which makes the collision head-on is

$$\begin{pmatrix} cT^* \\ X^* \\ Z^* \\ Y^* \end{pmatrix} = L \begin{pmatrix} cT \\ X \\ Z \\ Y \end{pmatrix}, \quad \begin{pmatrix} H^*/c \\ P_X^* \\ P_Z^* \\ P_Y^* \end{pmatrix} = L \begin{pmatrix} H/c \\ P_X \\ P_Z \\ P_Y \end{pmatrix},$$

where

$$L = \begin{pmatrix} 1/\cos\phi & -\sin\phi & -\tan\phi\sin\phi & 0 \\ -\tan\phi & 1 & \tan\phi & 0 \\ 0 & -\sin\phi & \cos\phi & 0 \\ 0 & 0 & 0 & 1 \end{pmatrix}.$$

It consists of a rotation in the X-Z plane by an angle ϕ and a boost to the direction of the rotated X (see Fig. 1). Here, ϕ is the half-horizontal crossing angle, and * indicates the quantities in the boosted frame. The reference particle $P_X = P_Y = 0$ and $H = cP_0$ is transformed into $P_X^* = P_Y^* = 0$ and $H^*/c = P_0^* = \cos\phi P_0$.

The $\mathbf{x}(0)$ is transformed to $\mathbf{x}^*(s^*)$ by

$$\begin{pmatrix} z^*(s^*) \\ x^*(s^*) \\ s^* \\ y^*(s^*) \end{pmatrix} = A^{-1}LA \begin{pmatrix} z(0) \\ x(0) \\ 0 \\ y(0) \end{pmatrix} = \begin{pmatrix} 1/\cos\phi & 0 & 0 & 0 \\ \tan\phi & 1 & 0 & 0 \\ 0 & -\sin\phi & \cos\phi & 0 \\ 0 & 0 & 0 & 1 \end{pmatrix} \begin{pmatrix} z(0) \\ x(0) \\ 0 \\ y(0) \end{pmatrix},$$

and

$$\begin{pmatrix} p_z^* \\ p_x^* \\ h^* \\ p_y^* \end{pmatrix} = B^{-1}LB \begin{pmatrix} p_z \\ p_x \\ h \\ p_y \end{pmatrix} = \begin{pmatrix} 1 & -\tan\phi & \tan^2\phi & 0 \\ 0 & 1/\cos\phi & -\tan\phi/\cos\phi & 0 \\ 0 & 0 & 1/\cos^2\phi & 0 \\ 0 & 0 & 0 & 1/\cos\phi \end{pmatrix} \begin{pmatrix} p_z \\ p_x \\ h \\ p_y \end{pmatrix}.$$

A world point with $s = 0$ is not necessarily transformed to $s^* = 0$. We need a transformation from $\mathbf{x}(0)$ to $\mathbf{x}^*(0^*)$; we thus perform the additional transformation

$$w_i^*(0^*) = w_i^*(s^*) - \frac{dw_i^*(0^*)}{ds^*} s^* = w_i^*(s^*) + h_i^* \sin\phi x(0).$$

Here w_i stands for (x, y, z), $h_i^* = \partial h^*/\partial p_i^*$, and $h^* = h(p_x^*, p_y^*, p_z^*)$. From Eq. (1), it is easy to show that

$$h^*(p_x^*, p_y^*, p_z^*; P_0^*) = \frac{1}{\cos^2\phi} h(p_x, p_y, p_z; P_0) = h(p_x^*, p_y^*, p_z^*; P_0^*).$$

We have thus obtained $\mathcal{L}$:

$$\begin{aligned} x^* &= \tan\phi z + [1 + h_x^* \sin\phi]x, \\ y^* &= y + \sin\phi h_y^* x, \\ z^* &= z/\cos\phi + h_z^* \sin\phi x, \\ p_x^* &= (p_x - \tan\phi h)/\cos\phi, \\ p_y^* &= p_y/\cos\phi, \\ p_z^* &= p_z - \tan\phi p_x + \tan^2\phi h. \end{aligned}$$

This map is quasisymplectic; the Jacobian of the transformation is $1/\cos^3\phi$. This is not a problem because the inverse factor $\cos^3\phi$ is applied by $\mathcal{L}^{-1}$ afterward. Within the ultrarelativistic approximation, the $\mathcal{L}$ is exact.

Beam-beam force: SBM.—The strong beam is cut into slices; each slice is represented by its $z^*(0^*)$ coordinate, denoted by $z^\dagger$. (We use $\dagger$ to indicate quantities of the strong beam.) At $s^* = 0$, we have $\sigma_z^\dagger = \sigma_z/\cos\phi$. The first and second moments of the particle distribution at the locations of the slices are (only terms linear with respect to dynamical variables in $\mathcal{L}$ are taken)

$$\begin{aligned} &X^\dagger = \sin\phi z^\dagger, \quad Y^\dagger = 0, \quad P_x^\dagger = 0, \quad P_y^\dagger = 0, \\ &P_z^\dagger = 0, \quad \Sigma_{11}^\dagger = \Sigma_{11}, \quad \Sigma_{22}^\dagger = \Sigma_{22}/\cos^2\phi, \\ &\Sigma_{33}^\dagger = \Sigma_{33}, \quad \text{and } \Sigma_{44}^\dagger = \Sigma_{44}/\cos^2\phi. \end{aligned}$$

The SBM is described in detail in Ref. [5]. It can be represented by a Hamiltonian $H = H_{bb}(\mathbf{x}^*)\delta(s^*)$, where H_{bb} is defined implicitly by

$$\exp{:}H_{bb}{:} = \prod_{z^\dagger} \exp{:}F(\mathbf{x}^*, z^\dagger){:}\ .$$

Here the Lie algebra notation [7] is used: $F(\mathbf{x}^*, z^\dagger)$ describes the interaction of a particle in the weak beam with a slice having $z^\dagger$. It is applied such that a particle collides first with the slice with the largest $z^\dagger$ and then with the next largest and so on. Here

$$F(\mathbf{x}^*; z^\dagger) = n^* U(X^*, Y^*; \Sigma_{11}^\dagger(S), \Sigma_{33}^\dagger(S)),$$

where n^* is the number of particles in the slice, $S = S(z^*, z^\dagger) = (z^* - z^\dagger)/2$ is the value of s^* for the real collision, $X^* = x^* + p_x^* S - X^\dagger(z^\dagger)$, and $Y^* = y^* + p_y^* S - Y^\dagger(z^\dagger)$.

We assume the transverse distribution of each slice is Gaussian so that the electromagnetic potential U is

$$U(x,y;\Sigma_{11},\Sigma_{33}) = -\frac{r_e}{\gamma_0}\int_0^\infty \frac{\exp[-x^2/(2\Sigma_{11}+u) - y^2/(2\Sigma_{33}+u)]}{\sqrt{2\Sigma_{11}+u}\sqrt{2\Sigma_{33}+u}}\,du\,.$$

Here r_e is the classical electron radius, and γ_0 is the γ associated with P_0. In a simulation, the longitudinal slices are positioned in such a way that each slice represents the same number of particles [5]. Note than in applying the kick to a test particle, we should use $\Sigma^\dagger_{11}$ and $\Sigma^\dagger_{33}$ at $S(z^*, z^\dagger)$: $\Sigma^\dagger_{11}(S) = \Sigma^\dagger_{11}(0) + 2\Sigma^\dagger_{12}(0)S + \Sigma^\dagger_{22}(0)S^2$, etc.

Arc $\mathcal{A}$.—We use a simple mapping for the arc. A coordinate $\mathbf{x}$ is transformed first by $\mathbf{x} \to \mathrm{diag}(V_x, V_y, V_z)\mathbf{x}$, where

$$V_{x,y} = \lambda_{x,y}\begin{pmatrix} \cos\mu_{x,y} & \beta^0_{x,y}\sin\mu_{x,y} \\ -\sin\mu_{x,y}/\beta^0_{x,y} & \cos\mu_{x,y}\end{pmatrix},$$

and

$$V_z = \begin{pmatrix} \cos\mu_z & -\beta^0_z\sin\mu_z \\ \lambda_z^2\sin\mu_z/\beta^0_z & \lambda_z^2\cos\mu_z\end{pmatrix},$$

with $\lambda_{x,y,z} = \exp(-1/T_{x,y,z})$. Here the T's are the damping times expressed in number of turns. Then we apply [5]

$$x \to x + \sigma^0_x\sqrt{1-\lambda_x^2}\,\hat{r}_1\,, \quad p_x \to p_x + \sigma^0_{p_x}\sqrt{1-\lambda_x^2}\,\hat{r}_2\,,$$
$$y \to y + \sigma^0_y\sqrt{1-\lambda_y^2}\,\hat{r}_3\,, \quad p_y \to p_y + \sigma^0_{p_y}\sqrt{1-\lambda_y^2}\,\hat{r}_4\,,$$
$$p_z \to p_z + \sigma^0_z\sqrt{1-\lambda_z^4}\,\hat{r}_5\,,$$

where the $\hat{r}$'s are Gaussian random numbers with $\langle\hat{r}\rangle = 0$ and $\langle\hat{r}^2\rangle = 1$, representing the radiation excitations.

Simulation.—We performed a weak-strong simulation using the set of parameters listed in Table I. We tracked 50 particles for 10 000 turns and accumulated data for beam sizes and the largest particle amplitudes. For the present parameters, the case with five slices gave results almost identical with those using more slices.

For the value $\eta_{x,y} = 0.01$ of the nominal beam-beam parameter, the beam sizes are shown in Fig. 2. For $\phi = 0$, the peaks indicate the resonances (from left to right) $n(\nu_x - \eta_x/2) + m(\nu_y - \eta_y/2) + l\nu_z =$ integer for $(n,m,l) =$ $(0,2,-1)$, $(0,2,-2)$, $(2,-2,-1)$, $(2,-2,0)$, $(0,4,0)$, $(2,2,0)$, $(2,2,-1)$, $(0,2,2)$, $(0,2,1)$, and $(0,2,0)$. Here $\nu_{x,y,z}$ are the tunes. For $\phi = 5$ mrad, the major difference is that $(1,2,0)$ and $(1,-2,0)$ appear. The latter two resonances are not SB resonances and are stronger for larger ϕ. These are induced by the nonlinear terms in $\mathcal{L}$ and $\mathcal{L}^{-1}$.

Letting $\eta_{x,y} = 0.05$, we compare results for several values of ϕ (see Figs. 3 and 4). It appears that the effects of ϕ on σ's [Figs. 3 and 4(a)] and amplitudes [Fig. 4(b)] increase with ϕ at first but decrease for larger ϕ. This is quite contrary to what is expected from Piwinski's formalism [2].

TABLE I. Standard parameters.

Emittances	(ϵ_x, ϵ_y)	$(2\times10^{-8}, 2\times10^{-10})$ m
Betatron functions at IP	(β^0_x, β^0_y)	(1, 0.01) m
Bunch length	σ_z	0.01 m
Relative energy spread	σ_ϵ	10^{-3}
Tunes	(ν_x, ν_z)	(0.2, 0.08)
Damping times	(T_x, T_y, T_z)	(2000, 2000, 1000) turns

Discussion.—To understand this discrepancy, it seems useful to consider the luminosity L and effective beam-beam parameter ξ_y in the boosted frame. Including the hourglass [8] and the beam-tilt effects, but excluding the dynamical effects, we define

$$R_L = \frac{L}{L_0} = \sqrt{\frac{2}{\pi}}\,ae^b K_0(b)\,, \qquad (2)$$
$$a = \frac{\sigma^*_y}{\sqrt{2}\,\sigma^*_z\sigma^*_{p_y}}\,, \quad b = a^2\left[1 + \left(\frac{\sigma^*_z}{\sigma^*_x}\tan\phi\right)^2\right],$$

and

$$R_\xi = \frac{\xi_y}{\eta_y} = \int dz^\dagger \rho(z^\dagger)\sqrt{1+(S/\beta^0_y)^2} \times f_y(z^\dagger\tan\phi, \sigma^*_x(S), \sigma^*_y(S))\,, \qquad (3)$$

where L_0 is the luminosity without hourglass reduction or tilt effect, ρ is the longitudinal distribution function of the strong beam, K_0 is a Bessel function, and $f_y(x,\sigma_x,\sigma_y)$ is Montague's reduction factor [9] of ξ_y for an off-center particle, which falls quite rapidly with ϕ. These are shown in Fig. 4(c). For small ϕ, R_ξ is larger than 1 due to the hourglass effect which makes the beam-beam interaction more serious. This decreases rapidly for larger ϕ. At the same time, R_L also decreases but less rapidly.

The essential difference from Piwinski's formalism [1] is the inclusion of the bunch-length effects by using several slices. In fact, if we use only one slice, the effect grows almost proportionally to ϕ and does not decrease. From Eqs. (2) and (3), it seems that two parameters are important: $R = \sigma_z/\beta^0_y$ and $\Phi = \phi\sigma_z/\sigma_x$ (Piwinski angle). For $R \gtrsim 1$, the hourglass effect is important even for $\phi = 0$ [3]. When $\Phi \gtrsim 1$, the tilt effect is important.

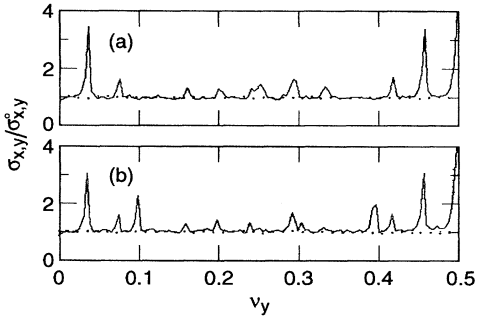

FIG. 2. σ_y/σ^0_y (solid) and σ_x/σ^0_x (dotted) vs ν_y for (a) $\phi = 0$ mrad and (b) $\phi = 5$ mrad, with $\eta = 0.01$.

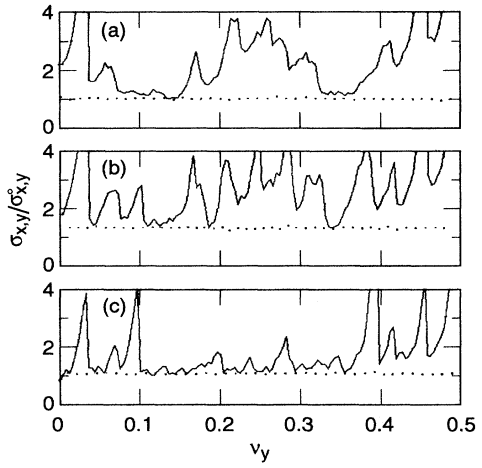

FIG. 3. σ_y/σ_y^0(solid) and σ_x/σ_x^0 (dotted) vs ν_y for (a) ϕ = 0 mrad, (b) ϕ = 5 mrad, and (c) ϕ = 20 mrad, with η = 0.05.

Piwinski's formalism worked well for DORIS where $R \ll 1$ and $\Phi \simeq 0.5$ (DORIS used vertical crossing, so σ_x is replaced by σ_y in Φ). In Pinwinski's formalism, R_ξ and R_L decrease in the same manner, because σ_x is simply replaced by an effective value of σ_x [1].

From simulation results shown above, and from results with several other sets of parameters, it seems that σ's and the maximum amplitudes become largest at around $\Phi = \frac{1}{2}$, and they become almost nominal values for $\Phi \gtrsim 1$.

A large ϕ ($\Phi \gtrsim 1$) might have several merits for high luminosity rings. (1) Luminosity reduction is only of geometrical origin: Compared to $\phi = 0$, R_L is small, but R_ξ is even smaller, so that the beam blowup is less serious. Since L is proportional to $1/(\sigma_x\sigma_y)$, it has a second maximum at $\Phi \sim 1$. In the example used in Fig. 3, as a function of Φ, $L(0)/L_0 = 86\%$, $L(0.5)/L_0 = 31\%$, and $L(1.13)/L_0 = 50\%$. (For shorter bunches, this merit becomes less remarkable but still exists. For $\sigma_z = \beta_y^0/2$ with the other parameters unchanged, for example, the maximum occurs at around $\Phi = 1.4$ and $L/L_0 = 56\%$.) (2) If we also use the crab crossing [10], the geometrical reduction of the luminosity might be recovered. Even without it, the loss of the luminosity relative to $\phi = 0$ is less than one half. (3) The beam separation around the IP is easier. (4) The good region in the tune plane is much wider (see Fig. 3).

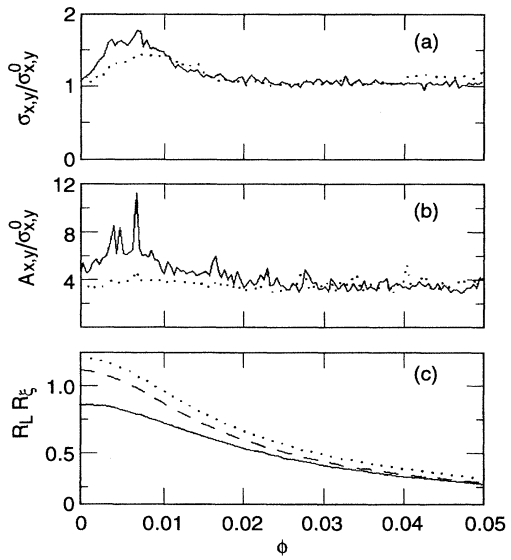

FIG. 4. The ϕ dependence of (a) σ_y/σ_y^0 (solid) and σ_x/σ_x^0 (dotted), (b) A_x (solid) and A_y (dotted), the horizontal and vertical maximum amplitudes being normalized to $\sigma^0_{x,y}$, and (c) the luminosity reduction factor R_L (solid), the ξ reduction factor R_ξ for $z = 0$ particle (dashed), and the same for $z = \sigma_z$ particle (dotted). Vertical tune ν_y is 0.15. For the present set of parameters, ϕ = 10 mrad corresponds to $\Phi = 0.707$.

The rate of falloff of the beam size with ϕ depends a little on the tunes. At some resonances, in particular, the beam sizes remain large. These points can be avoided easily.

The author wishes to thank M. Furman, H. Moshammer, and K. Oide for valuable discussions. R. Siemann is gratefully acknowledged for useful comments and careful reading of the manuscript. He also thanks the members of the group of R. Ruth at SLAC for their hospitality. This work was supported by Department of Energy Contract No. DE-AC03–76SF00515.

*On leave from KEK, National Laboratory for High Energy Physics, Tsukuba, Ibaraki 305, Japan.

[1] A. Piwinski, DESY Report No. DESY 77/18, 1977.

[2] For example, N. Toge, in *Proceedings of the International Workshop on B Factories, KEK, 1992,* edited by E. Kikutani and T. Matsuda (SLAC, Stanford University, Springfield, 1992) [KEK Report No. 93-7 (1993)].

[3] S. Krishnagopal and R. Siemann, Phys. Rev. D **41**, 2312 (1990).

[4] D. Sagan, R. Siemann, and S. Krishnagopal, in *Proceedings of the Second European Accelerator Conference, Nice, 1990* (EPS, Petit-Lancy, 1991), p. 1649; D. V. Pestrikov, KEK Report No. 93-16, 1993. These papers discussed the same effect, but it is not clear whether their formalisms apply for large ϕ.

[5] K. Hirata, H. Moshammer, and F. Ruggiero, Part. Accel. **40**, 205 (1993).

[6] J. Augustin, Orsay Report No. 36-69, 1969; K. Oide (private communication).

[7] A. J. Dragt, in *Physics of High Energy Particle Accelerators,* edited by R. A. Carrigan, F. R. Huson, and M. Month AIP Conf. Proc. No. 87, (AIP, New York, 1982), p. 147.

[8] G. E. Fischer, SLAC Report No. SPEAR-154, 1972; SPEAR Storage Ring Group, IEEE Trans Nucl. Sci. **NS-20**, 838 (1973); M. Furman, *Proceedings of the IEEE Particle Accelerator Conference, New York, 1991* (IEEE, New York, 1991), p. 422.

[9] B. W. Montague, CERN Report No. CERN/ISR-GS/75-36, 1975.

[10] K. Oide and K. Yokoya, Phys. Rev. A **40**, 315 (1989).